

Acetylene π -Coordination, Slippage to σ -Coordination, and 1,2-Hydrogen Migration Taking Place on a Transition Metal. The Case of a Ru(II) Complex As Studied by Experiment and ab Initio Molecular Orbital Simulations

Yasuo Wakatsuki,^{*,†} Nobuaki Koga,[‡] Hiroshi Yamazaki,[§] and Keiji Morokuma^{||}

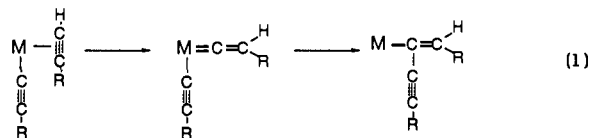
Contribution from The Institute of Physical and Chemical Research (RIKEN), Wako, Saitama 351-01, Japan, Department of Chemistry, School of Informatics and Sciences, Nagoya University, Chikusa, Nagoya 464-01, Japan, Department of Chemistry, Faculty of Science and Engineering, Chuo University, Kasuga, Bunkyo, Tokyo 112, Japan, and Cherry L. Emerson Center for Scientific Computing and Department of Chemistry, Emory University, Atlanta, Georgia 30322

Received April 15, 1994[®]

Abstract: The behavior of an acetylene molecule in the coordination sphere of transition metals has been probed by the reactions of $\text{RuX}_2(\text{PPh}_3)_3$ ($\text{X} = \text{Cl}, \text{Br}$) with *tert*-butylacetylene to give vinylidene complexes of the formula $\text{RuX}_2(\text{PPh}_3)_2(\text{C}=\text{CH}^t\text{Bu})$. IR and NMR data have indicated that the initial product of this reaction is a mixture of two complexes each of which has a vinylidene unit and nonequivalent *cis*-bis(phosphine) ligands. In solution, these kinetic products gradually isomerize to the final *trans*-bis(phosphine) complex. The structure of this five-coordinated and thermodynamically stable complex ($\text{X} = \text{Br}$) was determined by X-ray crystallographic analysis to have a quasi trigonal-bipyramidal conformation with the two phosphines occupying axial positions. The potential surface for the transformation of coordinated acetylene to vinylidene was calculated by the ab initio molecular orbital method. The primary process was concluded to be a slippage of the $\eta^2\text{-CC}$ coordinated alkyne to the $\eta^2\text{-CH}$ coordinated complex via a transition state with an $\eta^1\text{-acetylene}$ and a side-on acetylene. The $\eta^2\text{-CH}$ complex undergoes 1,2-hydrogen migration within the acetylene unit, whose transition state is the highest point of the whole process, giving finally the thermodynamically metastable vinylidene complex with a *cis*-bis(phosphine). The isomeric vinylidene ruthenium(II) complex with *trans*-bis(phosphine) has been calculated to be the final product and thermodynamically most stable form of this reaction system. The role of the metal in the present rearrangement is discussed on the basis of the localized molecular orbital analysis of the key intermediates.

The electronic character and reactivity of organic compounds change, often dramatically, when they interact with transition metals. Since this phenomenon is strongly related to many catalyzed processes, clarification or understanding of this basic problem is an important topic for organometallic as well as theoretical chemists. The relative stability of acetylene and its isomeric vinylidene form provides a good and simple example: free vinylidene, $\text{:C}=\text{CH}_2$, has been the subject of a number of theoretical and physicochemical studies¹ and is proved nowadays to be ca. 44–47 kcal/mol less stable than acetylene, $\text{HC}\equiv\text{CH}$.^{1–3} In contrast, 1-alkyne to vinylidene tautomerization in the coordination sphere of a transition metal has proved to be a useful entry into vinylidene complexes, apparently with vinylidene being the more stable form in many transition-metal complexes.^{4,5} Such

isomerization on transition metal sometimes plays a key role in catalytic C–C coupling reactions: coupling of metal–alkynyl and alkyne carbons to form a metal-bound butenyne group is considered to proceed via prior isomerization of the 1-alkyne into the vinylidene form (eq 1). Recently, Bianchini and co-workers and we have shown that such C–C coupling indeed takes place in Ru(II)-catalyzed dimerization of 1-alkynes to *Z*-1,4-disubstituted enynes⁶ and *Z*-1,4-disubstituted butatrienes,⁷ respectively.



(4) (a) Bruce, M. I. *Chem. Rev.* **1991**, *91*, 197 and references therein. (b) Werner, H. *Angew. Chem., Int. Ed. Engl.* **1990**, *29*, 1077 and references therein.

(5) Höhn, A.; Werner, H. *J. Organomet. Chem.* **1990**, *382*, 255. (b) Werner, H.; Rappert, T.; Wolf, J. *Isr. J. Chem.* **1990**, *30*, 377. (c) Werner, H.; Stahl, S.; Kohlmann, W. *J. Organomet. Chem.* **1991**, *409*, 285. (d) Knaup, W.; Werner, H. *J. Organomet. Chem.* **1991**, *411*, 471. (e) Werner, H.; Höhn, A.; Schulz, M. *J. Chem. Soc., Dalton Trans.* **1991**, 777. (f) Schäfer, M.; Wolf, J.; Werner, H. *J. Chem. Soc., Chem. Commun.* **1991**, 1341. (g) Schneider, D.; Werner, H. *Angew. Chem.* **1991**, *103*, 710. (h) Werner, H.; Dirnberger, T.; Höhn, A. *Chem. Ber.* **1991**, *124*, 1957. (i) Werner, H.; Weinhand, R.; Knaup, W. *Organometallics* **1991**, *10*, 3967. (j) Werner, H.; Stark, A.; Schulz, M.; Wolf, J. *Organometallics* **1992**, *11*, 1126. (k) Rappert, T.; O.; Mahr, N.; Wolf, J.; Werner, H. *Organometallics* **1992**, *11*, 4156. (l) Werner, H.; Weber, B.; Nürnberg, O.; Wolf, J. *Angew. Chem., Int. Ed. Engl.* **1992**, *31*, 1025. (m) Nakanishi, S.; Goda, K.; Uchiyama, S.; Otsuji, Y. *Bull. Chem. Soc. Jpn.* **1992**, *65*, 2560. (n) Haquette, P.; Pirio, N.; Touchard, D.; Toupet, L.; Dixneuf, P. H. *J. Chem. Soc., Chem. Commun.* **1993**, 163.

(6) Bianchini, C.; Peruzzini, M.; Zanobini, F.; Frediani, P.; Albiati, A. *J. Am. Chem. Soc.* **1991**, *113*, 5453.

[†] Institute of Physical and Chemical Research (RIKEN).

[‡] Nagoya University.

[§] Chuo University.

^{||} Emory University.

[®] Abstract published in *Advance ACS Abstracts*, August 1, 1994.

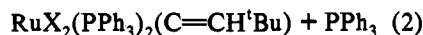
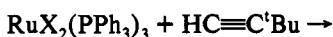
(1) (a) Krishnan, R.; Frisch, M. J.; Pople, J. A.; Schleyer, P. v. R. *Chem. Phys. Lett.* **1981**, *79*, 408 and references cited therein. (b) Osamura, Y.; Schaefer, H. F.; Gray, S. K.; Miller, W. H. *J. Am. Chem. Soc.* **1981**, *103*, 1904. (c) Carrington, T.; Hubbard, L. M.; Schaefer, H. F.; Miller, W. H. *J. Chem. Phys.* **1984**, *80*, 4347. (d) Gallo, M. M.; Hamilton, T. P.; Schaefer, H. F. *J. Am. Chem. Soc.* **1990**, *112*, 8714. (e) Petersson, G. A.; Tensfeldt, T. G.; Montgomery, J. A., Jr. *J. Am. Chem. Soc.* **1992**, *114*, 6133. (f) Paldus, J.; Cizek, J.; Jeziorski, B. *J. Chem. Phys.* **1989**, *90*, 4356. (g) Jensen, J. H.; Morokuma, K.; Gordon, M. S. *J. Chem. Phys.* **1994**, *100*, 1981.

(2) (a) Ervin, K. M.; Ho, J.; Lineberger, W. C. *J. Chem. Phys.* **1989**, *91*, 5974. (b) Ervin, K. M.; Gronert, S.; Barlow, S. E.; Gilles, M. K.; Harrison, A. G.; Bierbaum, V. M.; DePuy, C. H.; Lineberger, W. C.; Ellison, G. B. *J. Am. Chem. Soc.* **1990**, *112*, 5750.

(3) (a) Chen, Y.; Jonas, D. M.; Hamilton, C. E.; Green, P. G.; Kinsey, J. L.; Field, R. W. *Ber. Bunsen-Ges. Phys. Chem.* **1988**, *92*, 329. (b) Chen, Y.; Jonas, D. M.; Kinsey, J. L.; Field, R. W. *J. Chem. Phys.* **1989**, *91*, 3976.

Regarding the mechanism of the conversion of coordinated 1-alkynes to metal-bound vinylidenes, Antonova and co-workers have suggested that oxidative addition of the alkyne to give an alkynyl(hydrido)metal intermediate and subsequent 1,3-shift of the hydride from the metal to the β -carbon of the alkynyl might give the vinylidene complex.⁸ However, the extended Hückel calculations on $\text{Mn}(\text{C}_3\text{H}_5)(\text{CO})_2(\text{C}_2\text{H}_2)$ have suggested that the concerted intramolecular 1,3-hydrogen shift of the alkynyl-(hydrido)metal complex would have a very high activation energy and that a direct 1,2-hydrogen shift from the α - to β -carbon might be plausible.⁹ A series of works by Werner and co-workers appears to have provided experimental evidence to judge which of these pathways is more likely: they have shown that square-planar η^2 -alkyne complexes *trans*- $[\text{MCl}(\text{RC}\equiv\text{CH})(\text{P}^i\text{Pr}_3)_2]$ ($\text{M} = \text{Rh}, \text{Ir}$) rearrange to square-pyramidal alkynyl(hydrido) complexes $\text{MCl}(\text{P}^i\text{Pr}_3)_2(\text{H})(\text{C}=\text{CR})$, which on warming further isomerize to the vinylidene complexes *trans*- $[\text{MCl}(\text{C}=\text{CHR})(\text{P}^i\text{Pr}_3)_2]$.¹⁰ A little different from Antonova's proposal, the possibility of an intermolecular hydrogen shift between two alkynyl(hydrido)metal molecules has been pointed out.^{10c} More recently, Bianchini and co-workers have carried out kinetic studies on the rearrangement of a cationic alkynyl(hydrido)cobalt to its vinylidene form and proposed that it proceeds via a dissociative (nonconcerted) intramolecular 1,3-proton shift.¹¹

Obviously, too many possibilities exist once acetylene interacts with transition-metal complexes. Along with a diversity of configurations around the central metal, this problem is a challenge to theorists. Ab initio MO calculations on the acetylene-vinylidene rearrangement under the influence of a non-transition-metal atom have been reported,¹² but to our knowledge no ab initio theoretical report has appeared with transition-metal complexes. Seeking to model the key step (eq 1) in our catalytic dimerization described above,⁷ we have found that a ubiquitous ruthenium complex, $\text{RuX}_2(\text{PPh}_3)_3$ ($\text{X} = \text{Cl}$ or Br), reacts readily with *tert*-butylacetylene to give a stable vinylidene complex (eq 2). Since reaction 2 seemed rather simple and suitable for



mechanistic investigations, we decided to explore this system in detail with both experiment and ab initio theoretical calculations. NMR and X-ray analysis were used to determine the orientation of ligands around the central metal while theoretical calculations were successfully applied to elucidate the transition states and unstable key forms of the C2 unit under such circumstances.

Results and Discussion

(1) Reactions of $\text{RuCl}_2(\text{PPh}_3)_3$ and $\text{RuBr}_2(\text{PPh}_3)_3$ with $\text{HC}\equiv\text{C}^t\text{Bu}$. The complexes $\text{RuX}_2(\text{PPh}_3)_3$ ($\text{X} = \text{Cl}, \text{Br}$) react with excess $\text{HC}\equiv\text{C}^t\text{Bu}$ in benzene over 24 h at room temperature to give vinylidene complexes $\text{RuX}_2(\text{PPh}_3)_2(\text{C}=\text{CH}^t\text{Bu})$ (**1f**, $\text{X} = \text{Cl}$; **2f**, $\text{X} = \text{Br}$), whose spectral data have been previously reported.⁷

The X-ray structural analysis of **2f** (Figure 1a) showed that the molecule had a trigonal-bipyramidal structure with two

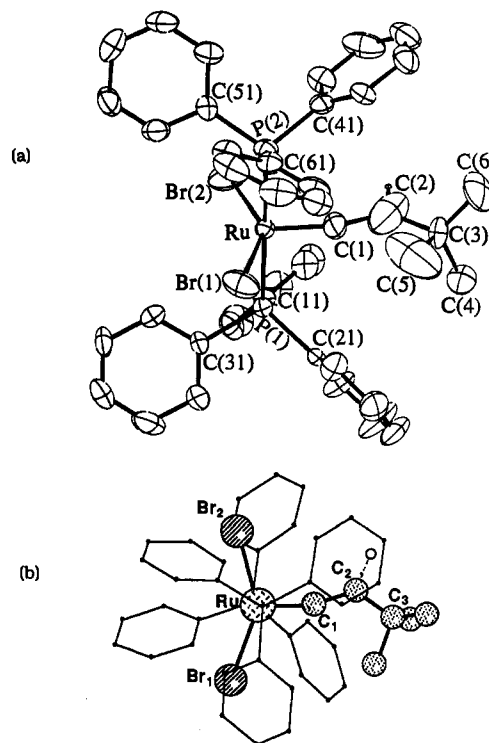


Figure 1. Molecular structure for **2f** with atomic-numbering scheme.

phosphines at axial positions but was deformed considerably toward square pyramidal with the vinylidene C_α at an apical position, the $\text{Br}-\text{Ru}-\text{Br}$ angle being $145.6(1)^\circ$. Though five-coordinated d^6 metal complexes have been calculated to adopt a square-pyramidal structure rather than a trigonal-bipyramidal one, the energy difference is small.¹³ The large deviation of the $\text{Br}-\text{Ru}-\text{Br}$ angle from linearity, with deformation toward the trigonal bipyramid, should be favored when steric repulsion between the Br's and the vinylidene moiety exists. The $\text{M}-\text{C}-\text{C}$ angles found in vinylidene complexes often deviate from linearity, but the present value of $161(2)^\circ$ is one of the largest.⁴ This is most likely due to severe steric repulsion between the phenyl rings of PPh_3 and the bulky ^tBu group at C_β , as easily seen from Figure 1b.

When the reaction of $\text{RuCl}_2(\text{PPh}_3)_3$ with $\text{HC}\equiv\text{C}^t\text{Bu}$ was stopped at an early stage, e.g. 15 min, by evaporating the excess alkyne and the solvent, a fine, red-brown powder was obtained. It showed an IR absorption at 1638 cm^{-1} , the typical $\nu(\text{C}=\text{C})$ region for a vinylidene ligand, but no peaks at all at $1700\text{--}2000\text{ cm}^{-1}$, the region for η^2 -coordinated alkyne or σ -alkynyl. The ^1H NMR spectrum in C_6D_6 showed the ^tBu resonance at δ 0.91 (broad s) and a proton absorption at 2.41 (broad t, $J = \text{ca. } 4\text{ Hz}$). When the NMR sample was allowed to stand at room temperature, the intensities of these peaks gradually decreased while the peaks due to **1f** at 0.79 (s, ^tBu) and 3.87 (t, $J = 4.4\text{ Hz}$, $=\text{CH}$) increased. The change was completed within 30 h. The ^{31}P NMR of the initial brown-red powder in C_6D_6 revealed that this was a mixture of almost equal amounts of two isomers, each of which had two nonequivalent phosphines: the spectrum exhibited two AB-type quartets centered at δ 46.5 ($J = 38\text{ Hz}$) and 34.4 ($J = 25\text{ Hz}$) with almost equal intensities. A small amount (ca. 5%) of a singlet at δ 27.2 due to **1f** was also observed, besides a singlet for free PPh_3 liberated as indicated in eq 2. When the NMR sample was allowed to stand at room temperature, the two quartets decreased as the singlet of **1f** at 27.2 increased with a rate almost equal to that observed for the change of the ^1H NMR spectra. On the basis of these spectral data, we have concluded that the

(7) Wakatsuki, Y.; Yamazaki, H.; Kumegawa, N.; Satoh, T.; Satoh, J. Y. *J. Am. Chem. Soc.* **1991**, *113*, 9604.

(8) (a) Nesmeyanov, A. N.; Aleksandrov, G. G.; Antonova, A. B.; Anisimov, K. N.; Kolobova, N. E.; Struchkov, Yu. T. *J. Organomet. Chem.* **1976**, *110*, C36. (b) Antonova, A. B.; Kolobova, N. E.; Petrovsky, P. V.; Lokshin, B. V.; Obezyuk, N. S. *J. Organomet. Chem.* **1977**, *137*, 55.

(9) Silvestre, J.; Hoffmann, R. *Helv. Chim. Acta* **1985**, *68*, 1461.

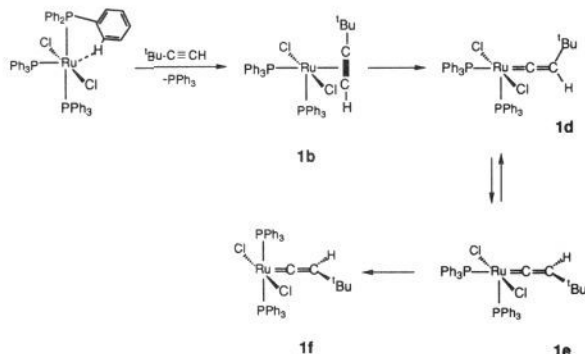
(10) (a) Wolf, J.; Werner, H.; Serhadli, O.; Ziegler, M. L. *Angew. Chem., Int. Ed. Engl.* **1983**, *22*, 414. (b) Höhn, A.; Otto, H.; Dziallas, M.; Werner, H. *J. Chem. Soc., Chem. Commun.* **1987**, 852. (c) Werner, H.; Alonso, F. J. G.; Otto, H.; Wolf, J. *Z. Naturforsch.* **1988**, *43b*, 722. (d) Werner, H.; Brekau, U. *Z. Naturforsch.* **1989**, *44b*, 1438. (e) Höhn, A.; Werner, H. *J. Organomet. Chem.* **1990**, *382*, 255.

(11) Bianchini, C.; Peruzzini, M.; Vacca, A.; Zanobini, F. *Organometallics* **1991**, *10*, 3697.

(12) Sakai, S.; Morokuma, K. *J. Phys. Chem.* **1987**, *91*, 3661.

(13) (a) Elian, M.; Hoffmann, R. *Inorg. Chem.* **1975**, *14*, 1058. (b) Daniel, C.; Koga, N.; Han, J.; Fu, X. Y.; Morokuma, K. *J. Am. Chem. Soc.* **1988**, *110*, 3773.

Scheme 1



initially formed brown-red powder consists of two isomers, **1d** and **1e**, depicted in Scheme 1. The ^1H NMR absorptions of the *tert*-butyl and vinylidene protons must have coincided between both isomers, since they are remote enough from the central metal, and the peaks are broad besides. Efforts to detect η^2 -alkyne complex **1b** have been unsuccessful: shorter reaction times resulted in a lower yield of the vinylidene complex with more unreacted material.

The reaction route we propose is illustrated in Scheme 1 and is fully consistent with the known structure of the starting $\text{RuCl}_2(\text{PPh}_3)_3$. The X-ray structural analysis of $\text{RuCl}_2(\text{PPh}_3)_3$ has shown that it has a slightly distorted square-pyramidal configuration.¹⁴ In the solid state, the metal weakly interacts with one of the phenyl hydrogens ($\text{Ru-H} = 2.59 \text{ \AA}$), but in solution it should open the coordination site. Though we have been unable to detect the η^2 -alkyne complex, it is reasonable to assume that coordination of the alkyne through the triple bond is involved in the present reaction sequence, since the alkyne π -complex is a thermodynamically stable species but *less* stable than the final vinylidene complex (*vide infra*). The bulky alkyne attacking this site will displace one of the neighboring triphenylphosphines to form an η^2 -CC alkyne complex **1b** with *cis*-bis(phosphine)s which quickly isomerizes to the vinylidene complex **1d** with the same metal configuration and with the *tert*-butyl group occupying the least crowded position. Our *ab initio* MO calculations on $\text{RuCl}_2(\text{PH}_3)_2(\text{C}=\text{CH}_2)$ have suggested that a rotational isomer **1e** is electronically favorable (*vide infra*). But the bulky *tert*-butyl group present in the actual reactant should prefer **1d** over **1e** in view of steric effects, thus equalizing the total energies of the two isomers giving a 1 to 1 mixture. Complex **1e** will slowly isomerize to the final product **1f**, which has been calculated to be the most stable form as described in the next section.

(2) **Molecular Orbital Calculations on the Intramolecular Rearrangement of $\text{RuCl}_2(\text{PH}_3)_2(\text{HC}\equiv\text{CH})$ to $\text{RuCl}_2(\text{PH}_3)_2(\text{C}=\text{CH}_2)$.** By means of *ab initio* molecular orbital calculations (GAUSSIAN 92 program¹⁵), we examined if there exists a reasonable path for the concerted intramolecular rearrangement of the π -coordinated acetylene complex to the vinylidene ruthenium complex. Throughout the calculations, except for complex **G** with a d^4 metal configuration (*vide infra*), the geometries of the stationary points were optimized at the MP2 (electron correlation by second-order Møller–Plesset perturbation) level using $[2s2p2d]/(3s3p4d)$ and the eight-valence-electron effective core potential of Hay and Wadt^{16a} for the metal, the 4-31G basis set¹⁷ for Cl and P, the 3-21G set¹⁸ for the H of PH_3 , the 4-31G* basis set¹⁹ for C, and the TZP set²⁰ for the H of the

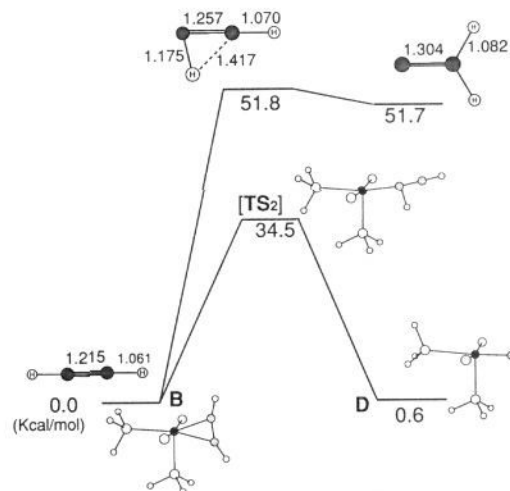


Figure 2. Comparison of the potential energy for the isomerization of acetylene to vinylidene in the free state (upper line) and in the ruthenium(II) complex (lower line). The units are \AA for atomic distances and kcal/mol for energies.

C_2H_2 moiety. To refine the energetics of the thus optimized structures, the MP2 energies were recalculated using the 16-valence-electron effective core potential^{16b} for Ru, which takes explicitly into account the outermost core orbitals, with the $[3s3p2d]/(5s5p4d)$ basis functions.

Before calculating the complexes, we examined the rearrangement of the free C_2H_2 unit. Many theoretical studies have already focused on the isomerization of free vinylidene ($:\text{C}=\text{CH}_2$) to acetylene ($\text{HC}\equiv\text{CH}$),¹ a reverse process of what we are considering here. Petersson, Tensfeldt, and Montgomery have recently provided a comparison of the various levels of *ab initio* theory for this isomerization reaction, including HF, MP2, and CCSD (coupled cluster single and double excitations) methods with STO-3G, 6-31G**, and 6-311 + G** basis sets.^{1c} The calculated geometries for vinylidene, acetylene, and the transition state have been found to be fairly insensitive to the level of theory in spite of the flat potential surface between the vinylidene and the transition state. In contrast, the height of the calculated barrier was very sensitive to the level of theory: Too large barriers were obtained unless electron correlation was induced; e.g., HF calculation with a large basis set gave a barrier for vinylidene to acetylene isomerization of 12.1 kcal/mol with an isomerization energy of -35.2 kcal/mol. Only a sophisticated method, the quadratic configuration interaction (QCI) calculations with large basis sets could reproduce the experimentally observed values of the reaction barrier (2 kcal/mol²) and the energy of isomerization (-47.4 ± 4.0 kcal/mol,² -44.4 ± 0.3 kcal/mol³). The results by MP2/6-31G* calculations have been found to be qualitatively satisfactory (barrier 1.07, isomerization energy -48.7 kcal/mol).^{1c} It appears, therefore, reasonable in view of economy to optimize the geometry by the MP2 method. The geometries and energies of free acetylene, vinylidene, and the transition state calculated by this methodology and with the basis sets we have employed as described above are shown by the upper line in Figure 2. The energy difference (0.1 kcal/mol) between the vinylidene form and the transition state, and the total isomerization energy (-51.7 kcal/mol) deviate by a few kcal/mol from the experimental values but are qualitatively, if not quantitatively, satisfactory.

Performing calculations on the C_2H_2 unit with the $\text{Ru}(\text{PH}_3)_2\text{Cl}_2$ moiety, we have found altogether six complexes, A–F, and

(14) La Placa, S. J.; Ibers, J. A. *Inorg. Chem.* **1965**, *4*, 778.

(15) Frisch, M. J.; Trucks, G. W.; Head-Gordon, M.; Gill, P. M. W.; Wong, M. W.; Foresman, J. B.; Johnson, B. G.; Schlegel, H. B.; Robb, M. A.; Replogle, E. S.; Gomperts, R.; Andres, J. L.; Raghavachari, K.; Binkley, J. S.; Gonzalez, C.; Martin, R. L.; Fox, D. J.; Defrees, D. J.; Baker, J.; Stewart, J. J. P.; Pople, J. A. *GAUSSIAN92*; Gaussian, Inc.: Pittsburgh, PA, 1992.

(16) (a) Hay, P. J.; Wadt, W. R. *J. Chem. Phys.* **1985**, *82*, 270. (b) Hay, P. J.; Wadt, W. R. *J. Chem. Phys.* **1985**, *82*, 299.

(17) Hehre, W.; Ditchfield, R.; Pople, J. A. *J. Chem. Phys.* **1972**, *56*, 2257.

(18) Binkey, J. S.; Pople, J. A.; Hehre, W. J. *J. Am. Chem. Soc.* **1980**, *102*, 939.

(19) (a) Ditchfield, R.; Hehre, W. J.; Pople, J. A. *J. Chem. Phys.* **1971**, *54*, 724. (b) Hariharan, P. C.; Pople, J. A. *Theor. Chim. Acta* **1973**, *28*, 213.

(20) (a) Dunning, T. H. *J. Chem. Phys.* **1971**, *55*, 716. (b) Dunning, T. H.; Hay, P. J. *Modern Theoretical Chemistry*; Plenum: New York, 1977; Vol. 2, p 1.

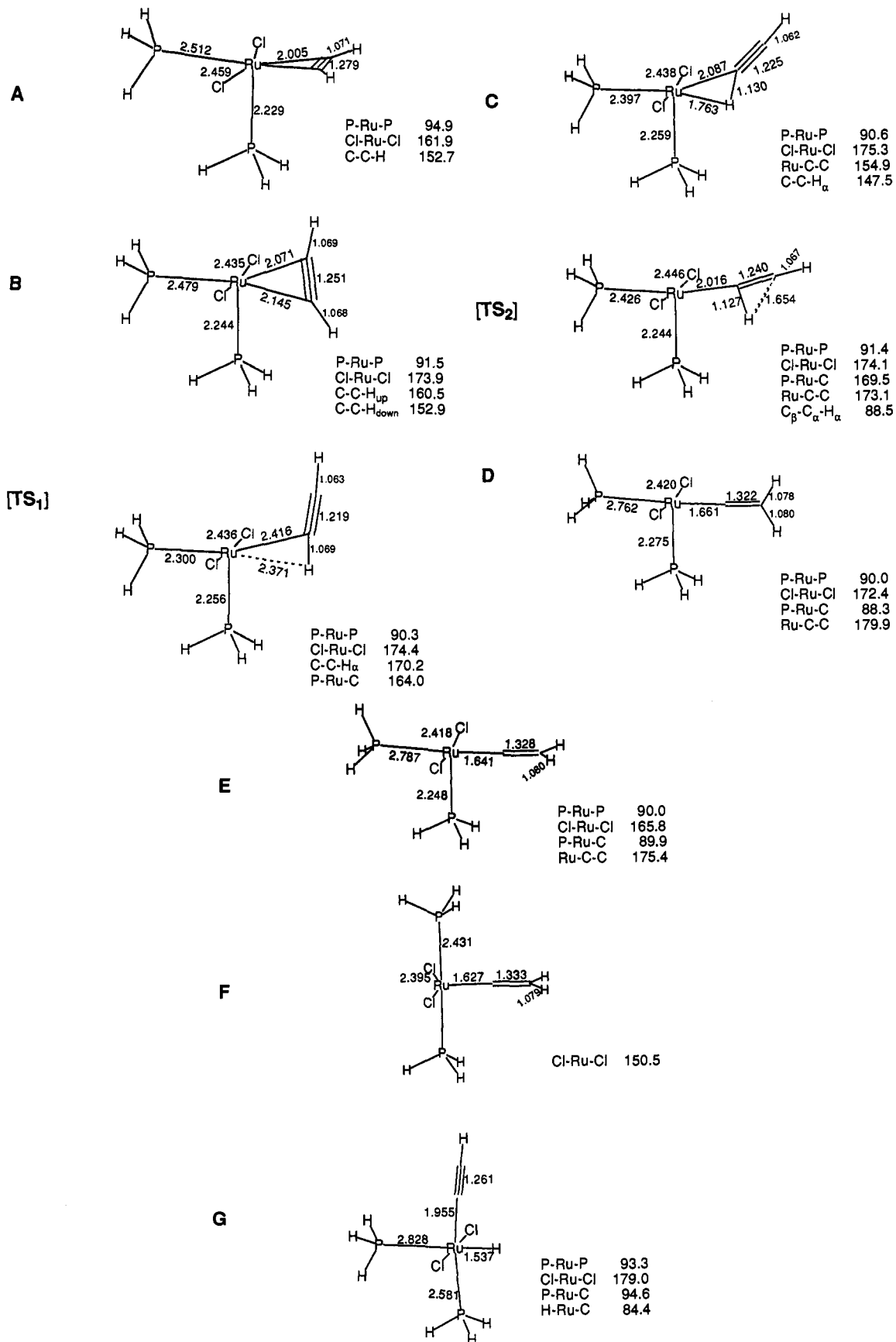


Figure 3. Calculated structures (in Å and deg) of $\text{RuCl}_2(\text{PH}_3)_2(\text{HC}\equiv\text{CH})$, $\text{RuCl}_2(\text{PH}_3)_2(\text{C}=\text{CH}_2)$, intermediates, and the transition states.

two transition states, [TS1] and [TS2], whose optimized structures are shown in Figure 3 while their relative energies are summarized in Figure 4. In the geometry optimizations, C_{2v} symmetry was assumed for the final product F, and C_3 symmetry, for the others.

Complexes A and B are rotational isomers of the η^2 -CC acetylene complex with *cis*-bis(phosphine) and *trans*-dichloride. Isomer B is less stable than A by 13.5 kcal/mol and is likely to be the transition state for this rotation. We could not find an

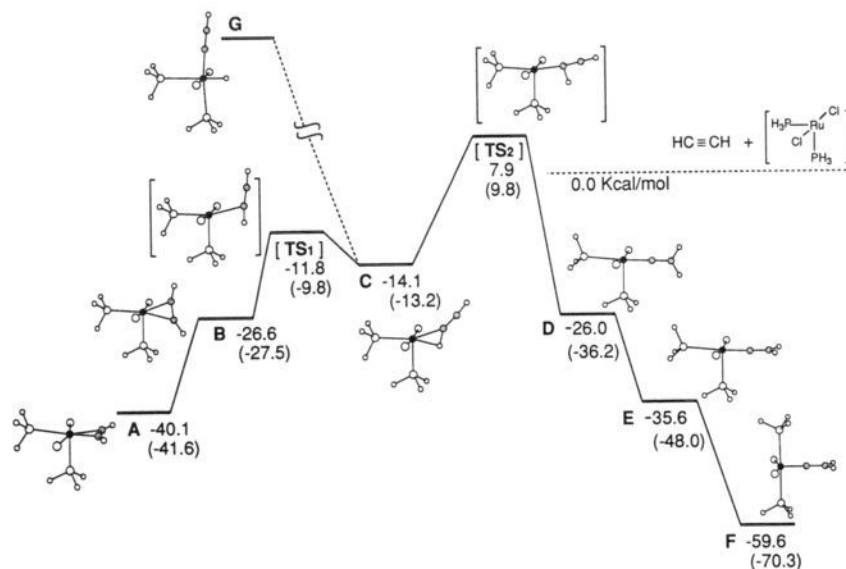
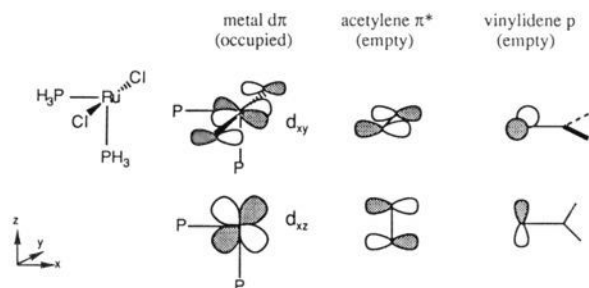


Figure 4. Energy diagram of $\text{RuCl}_2(\text{PH}_3)_2(\text{HC}\equiv\text{CH})$, $\text{RuCl}_2(\text{PH}_3)_2(\text{C}=\text{CH}_2)$, intermediates, and the transition states. Values in parentheses are energies calculated using the eight-valence-electron effective core potential for Ru.^{16a}

acetylene complex with *trans*-bis(phosphine) and *trans*-dichloride probably because of steric reasons. On the vinylidene complex side, however, such a conformation gives the most stable form **F**. As described in section 1, the primary vinylidene product must have two nonequivalent phosphines. Of the three different square-pyramidal geometries of vinylidene complexes which have nonequivalent *cis*-phosphines, forms **D** and **E** (*cis*-phosphines and *trans*-chlorides) are found to be energetically favorable (the other two have *cis*-phosphines and *cis*-chlorides). The rotational isomer **D**, rotation around the metal-carbon bond by 90°, was calculated to be 9.6 kcal/mol higher in energy than **E**. Similarly, the rotational isomer of **F** has been calculated to be more unstable than **F** by 11.4 kcal/mol, but it is not shown in Figure 4 for simplicity. These less stable rotational isomers are probably the transition states for the vinylidene rotation around the metal-carbon bond.

The more stable character of the η^2 -alkyne complex **A** compared to its isomer **B**, as well as the stability of the vinylidene **E** compared to the rotational isomer **D**, may be attributed to the efficiency of back-donation from the metal $d\pi$ orbitals. The importance of back-bonding in low-valent transition-metal alkene ($d\pi-\pi^*$)²¹ and vinylidene ($d\pi$ -empty p)²² complexes has been established. Calculations on the $\text{RuCl}_2(\text{PH}_3)_2$ fragment, which has *trans*-dichloride and *cis*-bis(phosphine) ligands, have shown that the d_{xy} orbital lies at a much higher energy level than does d_{xz} . The energy difference amounts to 0.09 au, and this can be traced back to an antibonding interaction of d_{xy} with the Cl p orbitals as illustrated below. The $d\pi$ orbital with higher orbital energy (d_{xy}) can more efficiently back-donate its electrons to the empty π^* orbital of the incoming alkyne or to the empty p orbital of the vinylidene ligand.²³



The vinylidene complexes with *cis*-phosphines are much less stable than the *trans*-phosphine isomers, and we had to fix the

P-Ru-P angle at 90° in the geometry optimizations of **D** and **E**. Without this restriction, they collapsed into the conformations with *trans*-phosphines and thus they are not the stationary points. In the real reaction (Scheme 1), however, corresponding *cis*-isomers **1d** and **1e** were observed, probably owing to steric reasons. Steric repulsion between the triphenylphosphine ligands and the *tert*-butyl group, as seen in Figure 1b, should make the energy of **1f** less stable than might be expected from the extremely stable calculation model **F**. It is very likely, therefore, that the *cis*-conformers like **D** and **E** are in stationary states in reaction 2, which involves bulky substituents.

With monosubstituted acetylenes, in particular taking into account the presence of the bulky *tert*-butyl group in our model reaction (Scheme 1), the acetylene complex **A** should be far less stable than the energy level expected from Figure 4 due to steric repulsion between the substituent and chloride. We may assume reasonably that the acetylene complex **B** is much more important, since the substituent can have the most free empty space when it is attached to the upper carbon. The crucial hydrogen migration should occur on the way from **B** to **D**, and the migrating hydrogen must be that at the lower carbon in **B**.

The transition state for the hydrogen migration step ([**TS**₂]) has been found, and the potential energy change in this process is compared in Figure 2 with that calculated for free acetylene. The C_2H_2 moiety in the [**TS**₂] complex adopts a similar structure to that calculated for the transition state of free C_2H_2 but is situated a little more to the alkyne side; the $\text{C}_\alpha\text{-H}_{\text{migrating}}$ distances of the free and complexed transition states are 1.175 and 1.127 Å and those of $\text{C}_\beta\text{-H}_{\text{migrating}}$ are 1.417 and 1.654 Å, respectively. The transition state in the complex is located early, reflecting the much smaller energy of isomerization. It is apparent from Figure 2 that, in the coordination sphere of the transition metal, the vinylidene lone pair can be stabilized by coordination to the metal. The large endothermic transformation from free acetylene to vinylidene is now thermoneutral in the complexed form. The lowering of the transition-state energy in the complex by ca. 17 kcal/mol can also be attributed to coordination of the lone-pair electrons.²⁴

Careful inspection of the path from **B** to [**TS**₂] has revealed further the presence of a η^2 -CH complex **C** and a small barrier

(21) Kitaura, K.; Sakaki, S.; Morokuma, K. *Inorg. Chem.* **1981**, *20*, 2292.

(22) Kostic, N. M.; Fenske, R. F. *Organometallics* **1982**, *1*, 974.

(23) The π^* (LUMO) of the acetylene fragment in **A** and empty p(LUMO) of the vinylidene fragment in **D** have energy levels higher than d_{xy} (HOMO) of the $\text{RuCl}_2(\text{PH}_3)_2$ fragment by 0.48 and 0.44 au, respectively.

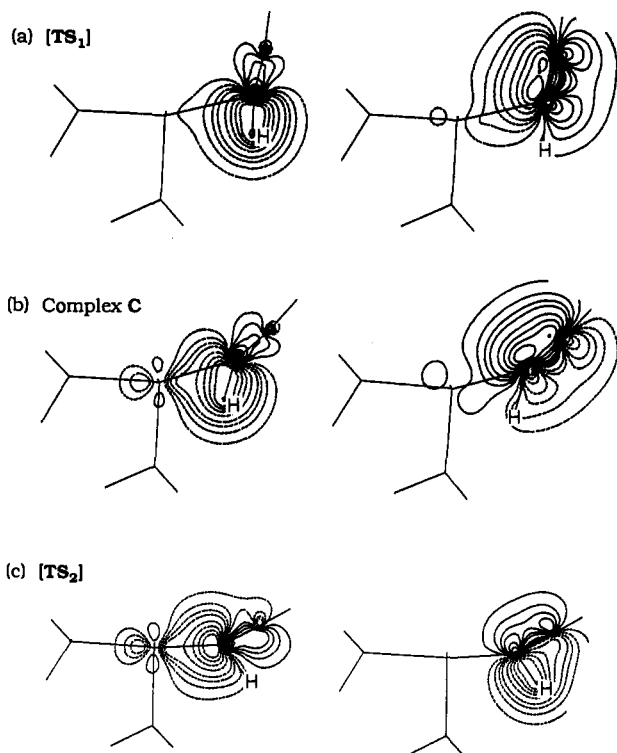


Figure 5. Localized molecular orbitals in the plane of P-Ru-CH-CH for intermediate C and the two transition states: left, C-H_α → lone pair; right, (C-C)π.

[TS₁] between B and C (Figure 4). The rearrangement of B to C is a slippage of the η²-CC acetylene complex to the η²-CH complex. In the transition state [TS₁] for this slippage, the metal interacts dominantly with only C_α and this interaction is very weak: the geometry of the C₂H₂ moiety deforms only slightly from the free acetylene and the Ru-C_α distance is as long as 2.4 Å (Figure 3).

Parts a-c of Figure 5 compare shapes of CH σ- and CC π-orbitals in the complexes [TS₁], C, and [TS₂]. These MO contour diagrams clearly demonstrate that the C_α-H_α σ-bond turns into the lone-pair orbital along the reaction coordinate while the in-plane CC π-orbital changes into the newly formed C_β-H_α σ-bond on going from [TS₁] to [TS₂]. The p orbital at C_α, which has been a part of the in-plane π-orbital, is left empty as the C_β-H σ-bond is being formed, and it should end up as the "empty p" orbital of the vinylidene to accept back-donation from the metal. It may be inferred that the migrating hydrogen behaves as a naked proton rather than a hydride. The migrating hydrogen leaves behind the lone pair of electrons which was originally used for the C_α-H σ-bond while it accepts the electrons, which originate from those of the in-plane CC π-orbital, to form the new C_β-H σ-bond. This view is in contrast to the concept proposed by Petersson et al.¹⁶ and Sakai et al.¹² for the free vinylidene → acetylene isomerization where the lone pair of the vinylidene is correlated with a π-orbital of acetylene and the migrating hydrogen has hydride character.²⁵ We conclude that the major role of Ru(II) in this rearrangement reaction is to interact with the C-H σ-bond first and then to promote its conversion to the

(24) As indicated in Figure 4, the energy level of [TS₂] is still ca. 8 kcal/mol higher than the dissociated state. This thermodynamics does not mean that the complex C dissociates before it goes over [TS₂]. We estimate that the transition energy needed for the dissociation of the acetylene unit from Ru is almost 50 kcal/mol, though we have not determined the exact transition-state geometry.

(25) Since acetylene keeps its interaction with Ru during the present reaction, the ambiguity of orbital transformation discussed by Petersson et al. is not met here. Our lone-pair LMO is an sp hybrid, different from their sp² hybrid arbitrarily chosen. We found that the lone-pair LMO at transition state for free acetylene can also be chosen as an sp hybrid, which is similar to that in the complexed form.

Table 1. Crystallographic Data for 2f

C ₄₂ H ₄₀ Br ₂ P ₂ Ru	V = 1876 Å ³
f _w = 867.6	Z = 2
cryst class: monoclinic	λ = 0.7107 Å
space group: P2 ₁	ρ _c = 1.534 g·cm ⁻³
a = 13.139(3) Å	μ(Mo Kα) = 6.65 cm ⁻¹
b = 15.276(3) Å	cryst size: 0.33 × 0.23 × 0.12 mm ³
c = 9.997(5) Å	R = 0.058
β = 110.74(3)°	R _w = 0.067

Table 2. Atomic Coordinates for 2f with Estimated Standard Deviations in Parentheses^a

atom	x	y	z
Ru	-3579(1)	-1348(0)	-6024(1)
Br1	-3187(1)	-128(1)	-7387(2)
Br2	-3947(1)	-2928(1)	-6035(2)
P1	-1676(2)	-1633(2)	-4980(3)
P2	-5505(2)	-1074(2)	-7101(3)
C1	-3582(11)	-958(14)	-4361(15)
C2	-3637(17)	-949(13)	-3024(22)
C3	-3458(12)	-175(10)	-2093(13)
C4	-2328(13)	-139(11)	-936(15)
C5	-3400(25)	608(25)	-3140(28)
C6	-4380(16)	87(21)	-1627(20)
C11	-1243(9)	-2658(8)	-3958(13)
C12	-1708(10)	-2856(10)	-2903(13)
C13	-1348(13)	-3574(10)	-2022(15)
C14	-550(13)	-4097(10)	-2186(16)
C15	-65(14)	-3917(10)	-3219(20)
C16	-445(12)	-3189(9)	-4117(16)
C21	-832(10)	-819(9)	-3730(13)
C22	-1064(13)	74(10)	-3987(15)
C23	-395(15)	682(10)	-3039(18)
C24	456(17)	420(12)	-1876(17)
C25	672(14)	-440(12)	-1577(19)
C26	47(12)	-1062(10)	-2511(17)
C31	-1069(9)	-1721(8)	-6362(12)
C32	-75(10)	-1377(12)	-6198(13)
C33	357(12)	-1446(12)	-7300(17)
C34	-257(13)	-1885(9)	-8569(15)
C35	-1251(12)	-2220(12)	-8713(14)
C36	-1663(11)	-2152(11)	-7613(13)
C41	-6228(9)	-1154(9)	-5860(13)
C42	-6751(13)	-442(11)	-5506(17)
C43	-7295(14)	-546(13)	-4506(18)
C44	-7281(12)	-1356(16)	-3865(16)
C45	-6846(13)	-2053(14)	-4302(17)
C46	-6275(13)	-1963(11)	-5250(15)
C51	-6264(9)	-1826(8)	-8549(12)
C52	-5726(10)	-2155(12)	-9430(13)
C53	-6283(12)	-2707(11)	-10568(15)
C54	-7382(12)	-2925(10)	-10837(15)
C55	-7891(11)	-2584(10)	-9943(15)
C56	-7338(10)	-2025(9)	-8831(13)
C61	-5852(9)	2(8)	-7981(12)
C62	-6332(12)	86(10)	-9439(14)
C63	-6514(12)	927(10)	-10068(16)
C64	-6214(12)	1675(11)	-9191(18)
C65	-5747(12)	1592(9)	-7814(19)
C66	-5529(11)	746(8)	-7115(14)

lone-pair orbital by accepting lone-pair electrons into a vacant metal d orbital.

Finally, the presence of a six-coordinate alkynyl(hydrido)-ruthenium(IV) intermediate in the present tautomerization reaction has been examined. If the oxidative addition of the acetylenic C-H takes place readily in the present system, the possibility of Antonova's 1,3-hydrogen shift⁸ or Werner's bimolecular hydrogen transfer^{10e} has to be considered. Since an octahedral d⁴ complex is expected to have two singly occupied d orbitals, the closed-shell MP2 calculations cannot be applied here. Assuming conservation of the spin state, we optimized the geometry of the oxidative addition product derived from C, i.e. RuCl₂(PH₃)₂(H)(C≡CH) (G) having a *trans*-dichloride and a *cis*-bis(phosphine), with singlet UHF calculations to a stationary

Table 3. Selected Interatomic Distances (Å) and Angles (deg) for **2f**

Distances			
Ru-Br1	2.469(2)	Ru-Br2	2.460(2)
Ru-P1	2.384(3)	Ru-P2	2.410(3)
Ru-C1	1.768(17)	C1-C2	1.36(3)
C2-C3	1.47(2)	C3-C4	1.53(2)
C3-C5	1.61(4)	C3-C6	1.50(3)
Angles			
Br1-Ru-Br2	144.81(7)	P1-Ru-P2	179.3(1)
Br1-Ru-P1	89.3(1)	Br1-Ru-P2	90.8(1)
Br2-Ru-P1	89.8(1)	Br2-Ru-P2	89.7(1)
C1-Ru-Br1	109.6(7)	C1-Ru-Br2	105.6(7)
C1-Ru-P1	90.0(5)	C1-Ru-P2	90.6(5)
Ru-C1-C2	161(2)	C1-C2-C3	125(2)

state shown in Figure 3. Due to the strong *trans* effect of the hydride ligand, the phosphine *trans* to it has a long metal-P distance of 2.8 Å. The energy was refined by the projected UMP2 method. To compare this energy level with the other complexes described above, we chose [TS₂], the highest point so far, as a reference and reoptimized its structure with the RHF level and then refined the energy with the MP2 calculation on the RHF optimized structure. The result indicated that the oxidative addition product **G** is very unstable, its UMP2 energy being ca. 67.5 kcal/mol higher than the MP2 energy of [TS₂]. Though the method of calculations used in the geometry optimization of **G** is different from others and hence exact comparison is not possible, it is qualitatively certain that the oxidative addition in the present system is thermodynamically very unfavorable, as indicated in Figure 4. The key complex **C** is the turning point of the reaction pathway, toward 1,2-hydrogen migration or to oxidative addition, the latter process being difficult if the metal changes from d⁶ to d⁴, as in the present case. For the d⁸ to d⁶ process, the oxidative addition should be just as easy as in the reaction of alkynes²⁶ or alkanes²⁷ with Rh(I) Wilkinson-type complexes.

(26) Wakatsuki, Y.; Koga, N.; Morokuma, K. Unpublished results.

Experimental Section

IR spectra were obtained with a Shimadzu IR-27G spectrometer using the KBr pellet method. NMR spectra were recorded on a JEOL JNM-GX-400 or GX-500 spectrometer using SiMe₄ (¹H) or H₃PO₄ (³¹P) as internal standard. The vinylidene complexes, **1f** and **2f**, were prepared as described previously.⁷ Single crystals of **2f** suitable for X-ray analysis were obtained by recrystallization from 1,2-dichloroethane/hexane.

X-ray Crystal Structure Determination of 2f. Crystal data are summarized in Table 1. X-ray measurements were carried out with a Nonius CAD4 four-circle diffractometer equipped with a graphite monochromator using ω - 2θ scans. Absorption correction was not made because deviations of F_o for axial reflections at $\chi = 90^\circ$ were within $\pm 5\%$. A total of 4712 unique reflections in the range $\pm h, \pm k, +l$ and $2^\circ < 2\theta < 55^\circ$ were measured, of which 3956 independent reflections having $I > 3\sigma(I)$ were used in subsequent analysis.

The structure was solved from direct and Fourier methods and refined by block-diagonal least squares with anisotropic thermal parameters in the last cycles for all non-hydrogen atoms. Hydrogen atoms for the six phenyl rings and the vinylic proton were placed in calculated positions, while those for the methyl groups were not located. In the refinements, unit weight was applied. The function minimized in the least-squares refinement was $\sum w(|F_o| - |F_c|)^2$. The handedness of the crystal was correctly established, since $R = 0.061$ for the opposite handedness. The computational program package used in the analysis was a UNICS 3 program system.²⁸ Neutral atomic scattering factors were taken from the *International Tables for X-ray crystallography*.²⁹ Final atomic parameters for the non-hydrogen atoms and important bond lengths and angles are given in Table 2 and 3, respectively.

Supplementary Material Available: Tables of positional and thermal parameters for **2f**, a full tabulation of bond distances and angles, and Cartesian coordinates of atom positions calculated for **A-F**, [TS₁], and [TS₂] (9 pages); a listing of observed and calculated structure factors (10 pages). This material is contained in many libraries on microfiche, immediately follows this article in the microfilm version of the journal, and can be ordered from the ACS; see any current masthead page for ordering information.

(27) (a) Koga, N.; Morokuma, K. *J. Phys. Chem.* **1990**, *94*, 5454; (b) *J. Am. Chem. Soc.* **1993**, *115*, 6883.

(28) Sakurai, T.; Kobayashi, K. *Rikagaku Kenkyusho Hokoku* **1979**, *55*, 69.

(29) *International Tables for X-Ray Crystallography*; Kynoch: Birmingham, England, 1976; Vol. 3, p 13.